



Minerva Access is the Institutional Repository of The University of Melbourne

Author/s:

Taouk, ML;Featherstone, LA;Taiaroa, G;Seemann, T;Ingle, DJ;Stinear, TP;Wick, RR

Title:

Exploring SNP filtering strategies: the influence of strict vs soft core

Date:

2025-01-01

Citation:

Taouk, M. L., Featherstone, L. A., Taiaroa, G., Seemann, T., Ingle, D. J., Stinear, T. P. & Wick, R. R. (2025). Exploring SNP filtering strategies: the influence of strict vs soft core. *Microbial Genomics*, 11 (1), pp.001346-. <https://doi.org/10.1099/mgen.0.001346>.

Persistent Link:

<https://hdl.handle.net/11343/359605>

License:

[CC BY-NC](#)

# Exploring SNP filtering strategies: the influence of strict vs soft core

Mona L. Taouk<sup>1,\*</sup>, Leo A. Featherstone<sup>2,3</sup>, George Tairaroa<sup>1</sup>, Torsten Seemann<sup>2,4</sup>, Danielle J. Ingle<sup>2,4</sup>, Timothy P. Stinear<sup>2,4</sup> and Ryan R. Wick<sup>2,4,\*</sup>

## Abstract

Phylogenetic analyses are crucial for understanding microbial evolution and infectious disease transmission. Bacterial phylogenies are often inferred from SNP alignments, with SNPs as the fundamental signal within these data. SNP alignments can be reduced to a 'strict core' by removing those sites that do not have data present in every sample. However, as sample size and genome diversity increase, a strict core can shrink markedly, discarding potentially informative data. Here, we propose and provide evidence to support the use of a 'soft core' that tolerates some missing data, preserving more information for phylogenetic analysis. Using large datasets of *Neisseria gonorrhoeae* and *Salmonella enterica* serovar Typhi, we assess different core thresholds. Our results show that strict cores can drastically reduce informative sites compared to soft cores. In a 10 000-genome alignment of *Salmonella enterica* serovar Typhi, a 95% soft core yielded ten times more informative sites than a 100% strict core. Similar patterns were observed in *N. gonorrhoeae*. We further evaluated the accuracy of phylogenies built from strict- and soft-core alignments using datasets with strong temporal signals. Soft-core alignments generally outperformed strict cores in producing trees displaying clock-like behaviour; for instance, the *N. gonorrhoeae* 95% soft-core phylogeny had a root-to-tip regression  $R^2$  of 0.50 compared to 0.21 for the strict-core phylogeny. This study suggests that soft-core strategies are preferable for large, diverse microbial datasets. To facilitate this, we developed *Core-SNP-filter* (<https://github.com/rrwick/Core-SNP-filter>), an open-source software tool for generating soft-core alignments from whole-genome alignments based on user-defined thresholds.

## Impact Statement

This study addresses a major limitation in modern bacterial genomics – the significant data loss observed in large datasets for phylogenetic analyses, often due to strict-core SNP alignment approaches. As bacterial genome sequence datasets grow and diversity increases, a strict-core approach can greatly reduce the number of informative sites, compromising phylogenetic resolution. Our research highlights the advantages of soft-core alignment methods that tolerate some missing data and retain more genetic information. To streamline the processing of alignments, we developed *Core-SNP-filter* (<https://github.com/rrwick/Core-SNP-filter>), a publicly available resource-efficient tool that filters alignments to informative and core sites.

Received 28 August 2024; Accepted 13 December 2024; Published 15 January 2025

**Author affiliations:** <sup>1</sup>Department of Infectious Diseases, The University of Melbourne at the Peter Doherty Institute for Infection and Immunity, Melbourne, Victoria, Australia; <sup>2</sup>Department of Microbiology and Immunology, The University of Melbourne at the Peter Doherty Institute for Infection and Immunity, Melbourne, Victoria, Australia; <sup>3</sup>Macroevolution and Macroecology Group, Research, School of Biology, Australian National University, Canberra, ACT, Australia; <sup>4</sup>Centre for Pathogen Genomics, The University of Melbourne, Melbourne, Victoria, Australia.

**\*Correspondence:** Mona L. Taouk, [taouk@student.unimelb.edu.au](mailto:taouk@student.unimelb.edu.au); Ryan R. Wick, [ryan.wick@unimelb.edu.au](mailto:ryan.wick@unimelb.edu.au); [rrwick@gmail.com](mailto:rrwick@gmail.com)

**Keywords:** core genome alignments; phylogenetic; SNP thresholds; temporal signal.

**Abbreviations:** RF, Robinson-Foulds; SNP, single-nucleotide polymorphism; WGS, whole-genome sequencing.

**Data statement:** Eight supplementary figures and three supplementary tables are available with the online version of this article.

001346 © 2025 The Authors



This is an open-access article distributed under the terms of the Creative Commons Attribution NonCommercial License. This article was made open access via a Publish and Read agreement between the Microbiology Society and the corresponding author's institution.

## DATA SUMMARY

All genomic sequence reads used in this study were already publicly available and accessions can be found in Dataset S1, available in the online version of this article. Supplementary methods and all code can be found in the accompanying GitHub repository: (<https://github.com/mtaouk/Core-SNP-filter-methods>).

## INTRODUCTION

Appropriately resolving the phylogenetic relationships between organisms is a fundamental aspect of many scientific disciplines, including ecology, microbiology and evolutionary biology [1]. Defining phylogenetic relationships using whole-genome sequencing (WGS) serves as a cornerstone application in clinical and public health settings for tracking the spread of pathogens and pinpointing outbreaks [2–7].

Conventionally, phylogenetic studies using WGS rely on reference-based techniques. In this approach, SNPs are identified for each sample by aligning sequencing reads against a reference genome and calling variants using bioinformatic tools such as *Snippy* (<https://github.com/tseemann/snippy>). These results are then combined to generate a whole-genome pseudoalignment ('alignment' for brevity) encompassing all relevant samples. If appropriate, recombination events and problematic areas of the genome can be masked from the alignment using tools such as *Gubbins* or *ClonalFrameML* [8, 9]. This alignment is then traditionally refined to produce what is known as a 'strict core', which includes only the SNP sites present in 100% of samples (see <https://github.com/sanger-pathogens/snp-sites> as an example). This strict-core approach is commonly used to generate the data required for phylogenetic inference, calculating SNP distances to infer the relatedness of genomes and patterns of transmission, and being the foundation for temporal phylogenetic inferences, especially in outbreak investigations and evolutionary studies [10–17].

The rapid decrease in sequencing costs has revolutionized our capacity for large-scale whole-genome analyses [18]. Contemporary bacterial studies now routinely involve WGS for thousands of samples, and public datasets number in the hundreds of thousands for some species. This necessitates revisiting methods for large-scale analyses, both within and across species. This is evidenced by studies employing methods other than whole-genome alignments to determine the genetic relatedness of isolates [19–22], with questions arising regarding the informativeness of alignments and the challenges of dealing with increasingly large datasets [23]. As more genomes are included, the strict-core alignment, consisting of sites present in all genomes, can only diminish in size due to the increasing likelihood of missing data in at least one genome, thereby reducing the overall resolution. This highlights the long-standing debate on the impact of excluding potentially informative sites [24, 25]. Some contemporary studies have addressed this concept by employing a 'soft-core' alignment by filtering the whole-genome alignment to include SNP sites present in fewer than all samples (<100%), although these approaches are not routine in bacterial genomics [6, 26, 27].

In this study, we evaluate the effectiveness of strict- and soft-core approaches for filtering whole-genome alignments and phylogenetic inferences using four priority bacterial species. To do so, we introduce *Core-SNP-filter* (<https://github.com/rrwick/Core-SNP-filter>), a tailored software tool that allows for efficient manipulation of large SNP alignments. Through these analyses, we aim to illuminate best practices for researchers seeking to accurately resolve phylogenetic relationships in bacteria.

## METHODS

### Development and implementation of Core-SNP-filter

To allow for the efficient filtering of core SNPs to user-defined thresholds, we developed *Core-SNP-filter*, which takes a FASTA alignment as input and outputs a reduced FASTA alignment based on core filtering settings. *Core-SNP-filter* accepts any FASTA alignment as input, including whole-genome alignments (such as output by *Snippy* or *SKA2*), gene-based alignments (such as output by *Roary* or *Panaroo*) and alignments with or without invariant sites. Additionally, we note that alignments without invariant sites and no missing or ambiguous data will remain unchanged by the filtering process.

*Core-SNP-filter* can discard invariant sites (controlled by the `-e` option) and non-core sites (controlled by the `-c` option). A site is determined to be invariant if the number of unique unambiguous bases (A, C, G or T) in that site is zero or one. A site is determined as the core if the fraction of bases in that site which are unambiguous exceeds the user-supplied value (e.g. `-c 0.95`). All characters other than the unambiguous bases (e.g. N, - and X) are treated the same (see Fig. 1 for an illustrated example).

*Core-SNP-filter* is implemented in Rust and is resource-efficient. It is available on GitHub (<https://github.com/rrwick/Core-SNP-filter>) with thorough usage instructions and a sample dataset.

### Large-scale genome analysis using PathogenWatch data

For two priority pathogens, *Neisseria gonorrhoeae* ( $n=11\,129$ ) and *Salmonella enterica* serovar Typhi ( $n=10\,991$ ), we downloaded the reads for all genomes available on PathogenWatch, an online database for processing and visualizing bacterial genome sequences in phylogenetic and geographical contexts with associated accessions and published studies (details

	60% core	80% core	100% core
leave invariant sites	<p>coresnpfilter -c 0.6</p> <p>sample 1: TTGAGAATTG-C                      sample 2: GAGAAANT-G-T                      sample 3: C-G--AACTG-C                      sample 4: --G--AGCGA-C                      sample 5: A-GAGAAC-G-C</p> <p style="text-align: center;">non-core</p>	<p>coresnpfilter -c 0.8</p> <p>sample 1: TTGAGAATTG-C                      sample 2: GAGAAANT-G-T                      sample 3: C-G--AACTG-C                      sample 4: --G--AGCGA-C                      sample 5: A-GAGAAC-G-C</p> <p style="text-align: center;">non-core</p>	<p>coresnpfilter -c 1.0</p> <p>sample 1: TTGAGAATTG-C                      sample 2: GAGAAANT-G-T                      sample 3: C-G--AACTG-C                      sample 4: --G--AGCGA-C                      sample 5: A-GAGAAC-G-C</p> <p style="text-align: center;">non-core</p>
exclude invariant sites	<p>coresnpfilter -e -c 0.6</p> <p style="text-align: center;">invariant</p> <p>sample 1: TTGAGAATTG-C                      sample 2: GAGAAANT-G-T                      sample 3: C-G--AACTG-C                      sample 4: --G--AGCGA-C                      sample 5: A-GAGAAC-G-C</p> <p style="text-align: center;">non-core</p>	<p>coresnpfilter -e -c 0.8</p> <p style="text-align: center;">invariant</p> <p>sample 1: TTGAGAATTG-C                      sample 2: GAGAAANT-G-T                      sample 3: C-G--AACTG-C                      sample 4: --G--AGCGA-C                      sample 5: A-GAGAAC-G-C</p> <p style="text-align: center;">non-core</p>	<p>coresnpfilter -e -c 1.0</p> <p style="text-align: center;">invariant</p> <p>sample 1: TTGAGAATTG-C                      sample 2: GAGAAANT-G-T                      sample 3: C-G--AACTG-C                      sample 4: --G--AGCGA-C                      sample 5: A-GAGAAC-G-C</p> <p style="text-align: center;">non-core</p>

**Fig. 1.** Schematic of the core filtering process at various thresholds. A visual depiction of how *Core-SNP-filter* processes sites with different settings. The highlighted sites are the ones that *Core-SNP-filter* will remove, i.e. the output will consist only of the non-highlighted sites. *Core-SNP-filter* uses  $\geq$  for core site assessment, e.g. with -c 0.8, a site with 4/5 unambiguous bases is considered core. All non-A/C/G/T characters (e.g. N and -) are treated equally. A site can be both invariant and non-core, and when both -e and -c are used, invariant sites are filtered first, so some non-core sites may shift to the invariant category.

in Supplementary Dataset, available in the online version of this article) [28]. In addition to being highly represented on PathogenWatch, these two species were selected because *N. gonorrhoeae* is naturally competent for genetic transformation and therefore represents a highly recombinogenic and diverse species, while *S. Typhi* has lower genetic diversity and less recombination [29, 30]. *Snippy* v4.6.0 was used with default settings to call variants, using *N. gonorrhoeae* NCCP11945 (accession: CP001050.1) and *S. Typhi* str. CT18 (accession: NC\_003198.1) as reference genomes [31, 32]. Genomes with more than 10% ambiguous bases (N characters) in their *Snippy* output sequence were excluded from downstream analyses (see Supplementary Methods).

For both species, we generated a series of alignments with progressively larger genome counts by incrementally adding genomes. Starting with an alignment of 25 genomes, we added genomes in increments of 25, creating alignments of 50, 75 and 100 genomes, and then continued with increments of 250 genomes, up to 10 000 genomes. Each alignment includes all genomes from the previous alignment, ensuring consistency across alignments and resulting in a total of 44 datasets with varying genome counts. For each of these 44 alignments, a core alignment was produced at thresholds of 50%, 60%, 70%, 80%, 90%, 95%, 96%, 97%, 98%, 99% and 100% using *Core-SNP-filter*, once removing invariant sites and a second time keeping all invariant sites. From each, the alignment length (number of remaining sites) was calculated.

This entire process was repeated ten times for each species, with a new random seed used for each repetition, and the reported results are the mean of all ten replicates. Additionally, for one set of *S. Typhi* alignments ranging from 25 to 2000 genomes, *Gubbins* v2.4.1 was used to identify regions of recombination [8]. For each alignment, *Core-SNP-filter* was used on the polymorphic sites identified by *Gubbins* to produce core alignments at thresholds of 50%, 60%, 70%, 80%, 90%, 95%, 96%, 97%, 98%, 99% and 100%.

To investigate the effect of changing between strict- and soft-core thresholds on related alignments, core SNP alignments were generated for 22 individual *N. gonorrhoeae* and 18 *S. Typhi* studies at both 100% and 95% thresholds [7, 16, 17, 33–69]. Genomic reads were downloaded from PathogenWatch corresponding to the published studies (Supplementary Methods). For each study, variants were called using *Snippy* with the *N. gonorrhoeae* NCCP11945 reference genome or *S. Typhi* str CT18 reference genome; a pseudoalignment was made with *Snippy-core*, and *Core-SNP-filter* was used to make 100% strict-core and 95% soft-core alignments. The number of variant sites in each core alignment was then counted and compared between the two thresholds. For each study alignment, the pairwise SNP distances between genomes were calculated with *snp-dists* v0.8.2 (<https://github.com/tseemann/snp-dists>).

## Evaluation of core thresholds for phylodynamics with public datasets

Four publicly available datasets were used to test core thresholds on a temporal regression analysis: 154 *Streptococcus pneumoniae* genomes [70], 192 *N. gonorrhoeae* genomes [17], 88 *Staphylococcus aureus* genomes [10] and 96 *Salmonella enterica* serovar Kentucky genomes [13]. These datasets were chosen because they each span a range of dates and contain a strong temporal signal, as demonstrated in their original publications.

For each dataset, we downloaded all available read sets and the reference genome used in the dataset's publication (see Supplementary Methods). Quality checks were performed on the reads from the *S. pneumoniae* dataset (excluding samples unable to assemble well, see Supplementary Methods), as these reads were from 2011 and of lower quality than the other three datasets. *Snippy* v4.6.0 was used with default settings to produce whole-genome pseudoalignments using the reference genome. *Snippy-core* was used to merge these into a combined alignment for each study. *Gubbins* v3.2.1 was used to generate a pseudoalignment with putative recombinant regions masked [8]. We then used *Core-SNP-filter* to produce an invariant-free alignment at each possible core threshold (e.g.  $0/n$ ,  $1/n$ ,  $2/n$ , ...  $(n-1)/n$ ,  $n/n$ ) for both the pre-*Gubbins* and post-*Gubbins* alignment.

We then used *IQ-TREE* v2.0.3 to produce three independent trees from each pseudoalignment using the TVM+F+ASC+R2 substitution model, the best-supported model identified by *IQ-TREE*'s inbuilt ModelFinder throughout these datasets [71]. Each tree was rooted by selecting the root position maximizing  $R^2$  for root-to-tip regression using *ape* v5.7.1 [72]. For each pseudoalignment/tree, we extracted the number of variant sites and  $R^2$  of the root-to-tip regression (a measure of the temporal signal strength for a strict molecular clock). We expect higher values of  $R^2$  at the 95% core threshold compared to the 100% threshold because reduced polytomy should lead to better fit in root-to-tip regression by informing the spread of root-to-tip distances on the y-axis. Robinson-Foulds (RF) distances were calculated using *phangorn* v2.12.1 to compare the topologies of phylogenies generated with a 100% strict-core threshold to phylogenies generated at each possible core threshold across each of the four datasets with three replicates [73, 74]. RF distances were normalized such that a value of one represents maximally dissimilar trees, while a value of zero represents identical topology.

## Benchmarking of Core-SNP-filter against similar tools

To evaluate the computational performance of *Core-SNP-filter*, we conducted benchmarking tests relative to three other tools: *Goalign* v0.3.7, *SNP-sites* v2.5.1 and *TrimAl* v1.4.1 [75–77]. We quantified the time and RAM required for two tasks: converting full alignments to no-invariant-site alignments and converting no-invariant-site alignments to 95% core alignments. *Core-SNP-filter* and *Goalign* can perform both tasks, while *SNP-sites* can only perform the first task and *TrimAl* can only perform the second. Each tool was cloned from GitHub and built from source code on a system equipped with an AMD EPYC 7742 CPU and 512 GB of RAM. The test dataset consisted of a 10 000-genome *S. Typhi* pseudoalignment, which was 4 809 037 bp in length and 47 GB in size. The sequences contained the characters -, A, C, G, T, N, a, c, g, t and n. Genome counts ranging from 10 to 10 000 were tested, spaced evenly on a logarithmic scale.

The benchmarking process involved subsampling the initial alignment to create datasets of varying genome counts. For each dataset, we used the tools to remove invariant sites and then to produce a 95% core alignment. Each test was repeated eight times, and the minimum time and RAM usage were recorded. MD5 checksums of the output files ensured consistency of results across different tools.

## Statistical analyses and data visualization

All statistical analyses were performed in *RStudio* v2022.12.0+353 using *R* v4.2.2. All figures were made using *ggplot2* v3.4.0.

# RESULTS

## Revisiting the appropriateness of strict-core filtering for large and diverse datasets

We evaluated the impact of core thresholds on alignment size and number of informative sites for phylogenetic analyses for two species with more than 10 000 publicly available genomes: *N. gonorrhoeae* and *S. Typhi*. For *S. Typhi*, we analysed 10 991 genomes collected between 1935 and 2020 from 95 countries, forming a geographically and temporally diverse dataset (accessions in Dataset S1). These genomes were sequentially subset into 44 alignments varying by number of genomes (see Methods for details). Similarly, for *N. gonorrhoeae*, 11 129 genomes collected between 1928 and 2018 from 62 countries were also subset into 44 alignments varying by number of genomes (accessions in Dataset S1).

For both *N. gonorrhoeae* and *S. Typhi*, the 100% strict core resulted in progressively fewer alignment sites as the number of genomes increased (Figs 2a, b and S1, Dataset S2). At all other core thresholds tested (50–99%), the number of sites remained stable as the number of genomes increased. For example, an alignment of 10 000 genomes at a strict threshold of 100% resulted in a mean of 256 124 and 633 715 sites for *N. gonorrhoeae* and *S. Typhi*, respectively, compared to a soft threshold of 95%, which resulted in a mean of 1 900 987 and 4 634 869 sites in *N. gonorrhoeae* and *S. Typhi*, respectively.

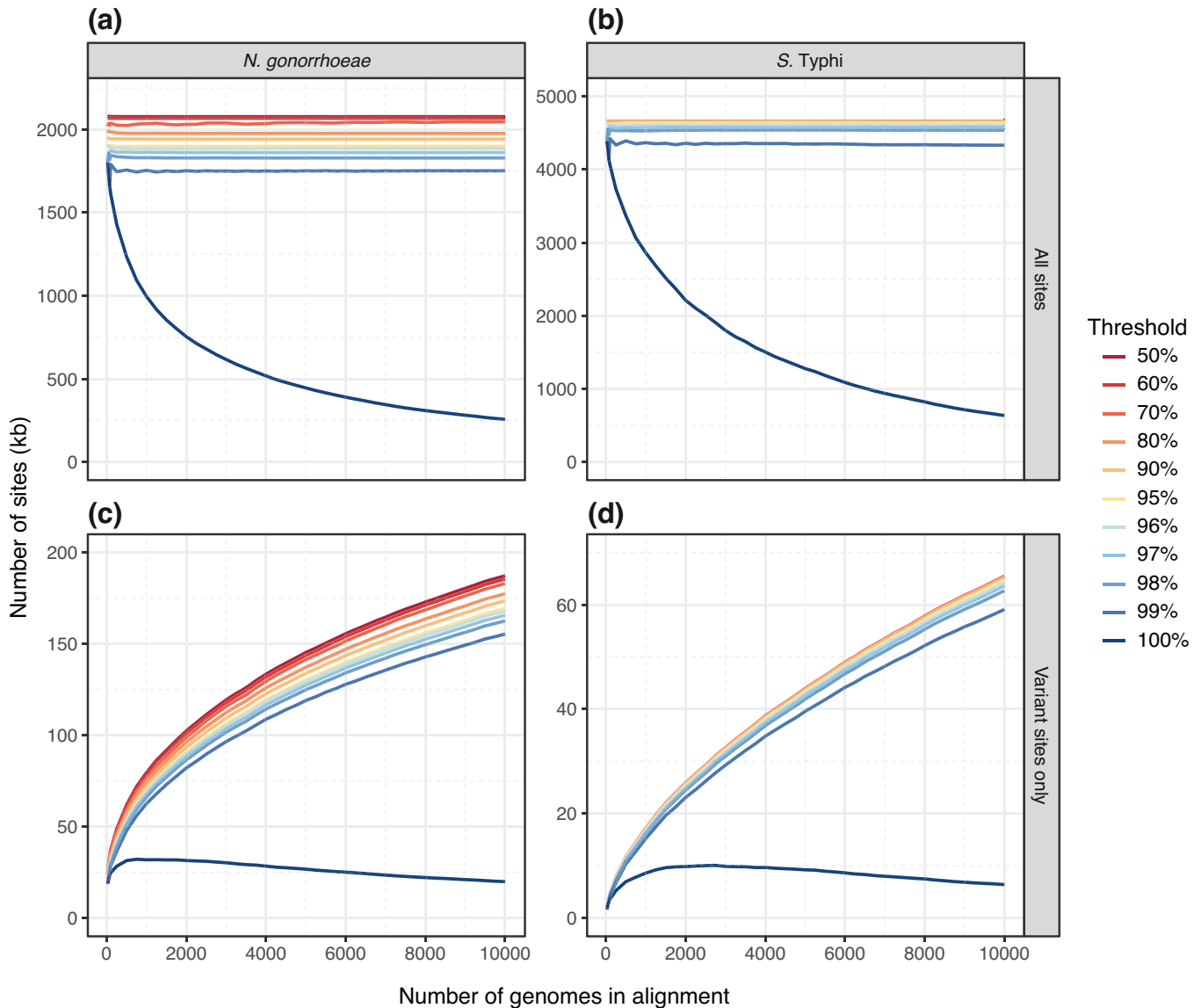


**Fig. 2.** Evaluation of core thresholds on alignment size and variant sites. The number of alignment sites (in kilobases) is plotted against the number of genomes included in each alignment (ranging from 25 to 10,000). Each alignment was processed at core thresholds ranging from 50% to 100% (indicated by line colour). (a) All sites in *Neisseria gonorrhoeae* alignments, (b) all sites in *Salmonella enterica* subspecies Typhi alignments, (c) variant sites only in *N. gonorrhoeae* alignments and (d) variant sites only in *Salmonella enterica* subspecies Typhi alignments. The number of sites was similar across different core thresholds, except for the 100% threshold, which resulted in far fewer sites, particularly at higher genome counts.

A similar trend was observed when considering variant sites. For both *N. gonorrhoeae* and *S. Typhi*, the 100% strict core resulted in drastically fewer variant sites compared to other thresholds at all alignment sizes (Fig. 2c, d). Except for the 100% strict core, the number of variant sites increased with the number of genomes at all tested thresholds, and the number of variant sites increased as the core threshold decreased. For example, an alignment of 10,000 genomes at a strict threshold of 100% resulted in a mean of 19,926 and 6,415 variant site outputs for *N. gonorrhoeae* and *S. Typhi*, respectively, compared to a soft threshold of 95%, which resulted in a mean of 169,409 and 64,711 variant site outputs in *N. gonorrhoeae* and *S. Typhi*, respectively. Similarly, after removing recombination, the 100% strict-core threshold produced 9,783 variant sites, whereas the 95% soft-core threshold yielded 24,703 variant sites in *S. Typhi* (Fig. S2). These findings indicate that considerably more evolutionary signals can be captured using soft-core approaches (<100%) compared to strict-core approaches (100%).

In genomic epidemiology, datasets from individual studies may exhibit reduced diversity and potential biases due to variable temporal, contextual and/or geographic sampling. To assess the potential impacts of varying core thresholds, we collated a set of *N. gonorrhoeae* ( $n=22$ ) and *S. Typhi* ( $n=18$ ) studies and generated alignments for each using both 100% and 95% thresholds (see

Methods) [7, 16, 17, 33–69]. For all but one study, the number of variant site outputs increased in the 95% threshold alignment compared to the 100% threshold alignment (Figs S3–S4 and Table S1–S2). In *N. gonorrhoeae*, large and diverse datasets particularly benefited from lowering the core threshold, as shown by Williamson *et al.* (2162 genomes), which had the highest increase in variant sites at 511.2% [7]. Other studies with substantial increases included Thomas *et al.* (639 genomes, 107.16%) and Alfsnes *et al.* (806 genomes, 122.76%) [16, 33]. Fifer *et al.* (97 genomes) and Kwong *et al.* (75 genomes) exhibited smaller increases of 8.59% and 6.16%, respectively, showing that smaller and/or less diverse datasets may see less benefit from lowering the threshold [40, 42]. Ezewudo *et al.* (18 genomes) showed no change in SNP sites, highlighting that for very small datasets lacking in diversity, threshold adjustments may not impact variant site counts [39]. A similar trend was observed in *S. Typhi*, where larger datasets showed more pronounced increases in variant sites at the 95% threshold. For instance, Wong *et al.* (1819 genomes) saw a large increase of 216.0% in variant sites, while da Silva *et al.* (3398 genomes) saw an increase of 79.6% [56, 69]. In contrast, smaller datasets like Guevara *et al.* (76 genomes) showed a modest increase from 1328 to 1886 variant sites, and Rasheed *et al.* (26 genomes) had minimal change from 19 to 20 sites [58, 66]. This cross-species analysis reinforces that lowering the core threshold can markedly increase variant site counts, especially in large, diverse datasets.

In addition to the observed differences in variant site counts, the 100% core threshold alignment resulted in a higher percentage of identical genome pairs (zero SNP distance) compared to the 95% core threshold alignment across all studies, except for three studies with no identical genomes in either alignment (Figs S5 and S6, Tables S1 and S2). For example, in the Williamson *et al.* dataset (*N. gonorrhoeae*), the proportion of identical genome pairs increased from 0.07% in the 95% core alignment to 2.43% in the 100% core alignment [7]. Similarly, in the Wong *et al.* dataset (*S. Typhi*), the percentage rose from 0.06 to 3.82% under the same comparison [69]. This trend suggests that strict-core alignments reduce genomic resolution, even though ambiguous ‘N’ bases are excluded from SNP counts.

### Appropriateness of using a strict-core threshold for small datasets with strong temporal signal

To investigate the effect of varying core thresholds in situations where removing certain sites might be beneficial – such as those inconsistent with the clonal frame of evolution or regions affected by recombination – we analysed four existing datasets. These datasets, characterized by a strong temporal signal and limited geographic diversity, provide an ideal context for assessing the appropriateness of different core thresholds for uncovering a stronger temporal signal, which is essential for subsequent phylodynamic analyses aiming to make epidemiological inferences from time-stamped genome sequences [78, 79]. Each dataset represents a different pathogen: *Streptococcus pneumoniae*, *N. gonorrhoeae*, *Salmonella* Kentucky and *Staphylococcus aureus* [10, 13, 17, 70]. For each, we generated both pre-*Gubbins* (unfiltered) and post-*Gubbins* (recombination-filtered) alignments, which were processed with core thresholds ranging from 50 to 100% (see Methods).

In general, recombination-filtered alignments had fewer variant sites at each core threshold across all four datasets (Fig. 3a). Like the results observed in the large datasets, the number of variant sites for all recombination-filtered alignments was generally consistent until a decrease as the core threshold approached 100% (Dataset S3). The unfiltered alignments had an overall higher number of variant sites, especially at lower core thresholds. Across all datasets, for both the recombination-filtered and unfiltered alignments, the lowest number of variant sites was observed in the 100% core threshold alignments. We identified specific instances in the unfiltered alignments, such as at 71% and 91% core thresholds for *Staphylococcus aureus* and at 78% core for *Salmonella* Kentucky, where a sharp decrease in variant sites occurred due to large regions of consistent sequence patterns across samples, rather than low-quality data. In each of these cases, the relevant genomic regions were masked by *Gubbins*, so these sharp decreases did not occur in the recombination-filtered alignments. Additionally, when comparing the tree topology generated from a 100% core threshold alignment to those from a 95% core threshold alignment, we observed some changes to the topology including more polytomous branching in the 100% core alignment, with other topological variation being minor (Figs S7 and S8, Table S3). This suggests that the evolutionary relationships between genomes were less resolved at the 100% core threshold.

Here,  $R^2$  is a measurement of the temporal signal in each dataset, which is essential for subsequent phylodynamic analyses aiming to estimate rates of epidemiological transmission. For the *N. gonorrhoeae* dataset, the  $R^2$  values remained relatively stable across all tested core thresholds, until a steep decline as the core threshold approached 100%, with the same trend being observed for both the recombination-filtered and unfiltered phylogenies (Fig. 3b, Dataset S3). Similarly, the *Streptococcus pneumoniae*  $R^2$  values remained relatively stable across core thresholds, until a steep decline as the core threshold approached 100%. For the *Streptococcus pneumoniae* dataset, the impact of removing recombination on the  $R^2$  values was more pronounced, with a mean  $R^2$  difference of 0.41 between the recombination-filtered and unfiltered phylogenies. In the case of the *Staphylococcus aureus* dataset, there was a noticeable difference between the  $R^2$  values for the recombination-filtered and unfiltered phylogenies. Across all core thresholds, the recombination-filtered *Staphylococcus aureus* phylogenies had very consistent  $R^2$  values, while the  $R^2$  values for the unfiltered *Staphylococcus aureus* phylogenies were much more varied and did not follow a discernible trend. However, at the 100% core threshold, both the recombination-filtered and unfiltered *Staphylococcus aureus* phylogenies had an  $R^2$  value of 0.95. Similarly, the *Salmonella* Kentucky dataset also showed relatively consistent  $R^2$  values across all tested core thresholds for the recombination-filtered phylogenies and more varied  $R^2$  values for the unfiltered phylogenies.

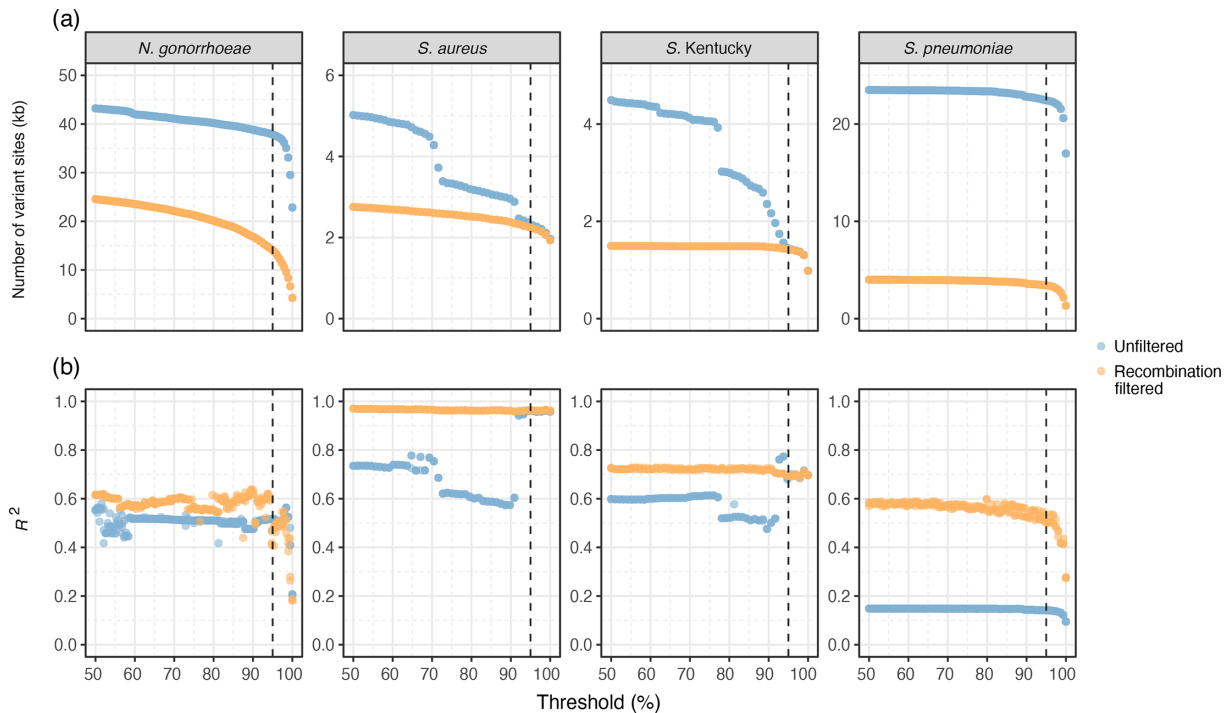


**Fig. 3.** Impact of core thresholds on phylogenetic and temporal signal across bacterial datasets. (a) The number of variant sites (in kilobases) at each genome threshold from 50% to 100% for four bacterial datasets: *Neisseria gonorrhoeae*, *Staphylococcus aureus*, *Salmonella enterica* subspecies Kentucky and *Streptococcus pneumoniae*. The variant sites are shown for both recombination-filtered (using *Gubbins*) and unfiltered alignments. (b) The  $R^2$  value from root-to-tip regression at each core threshold from 50% to 100% for phylogenetic trees constructed from the same four bacterial datasets, indicating the strength of the temporal signal. For all plots, the dotted line represents the 95% core threshold. Each dataset shows a steep decline in variant sites as the threshold approaches 100%, with *Neisseria gonorrhoeae* and *Streptococcus pneumoniae* also exhibiting a reduction in  $R^2$  as the threshold approaches 100%.

### Benchmarking Core-SNP-filter against existing tools

To evaluate the performance of *Core-SNP-filter* against three tools that perform related functions, *Goalign*, *SNP-sites* and *TrimAl*, we conducted benchmarking tests on two specific tasks: converting full alignments to no-invariant-site alignments and converting no-invariant-site alignments to 95% core alignments. *Core-SNP-filter* and *Goalign* can perform both tasks, whereas *SNP-sites* can only perform the first task, and *TrimAl* can only perform the second. These tools were chosen because they are written in fast, compiled programming languages: *Core-SNP-filter* in Rust, *Goalign* in Go, *SNP-sites* in C and *TrimAl* in C++.

There was a clear relationship between genome count and execution time for all tools and tasks (Fig. 4). For the task of removing invariant sites, *SNP-sites* was the fastest, with *Core-SNP-filter* taking about 1.5 times longer and *Goalign* taking about seven times longer (Fig. 4a). For the task of producing a 95% core alignment, *Core-SNP-filter* was the fastest, while *Goalign* and *TrimAl* took approximately four times longer (Fig. 4c). In terms of RAM usage, *Core-SNP-filter* consistently used a fixed amount of RAM regardless of genome count for both removal of invariant sites (mean: 51.8 MB) and generating the 95% core alignments (mean: 2.8 MB) (Fig. 4b, d). For the removal of invariant sites, both *Goalign*'s and *SNP-sites*' RAM usage increased with genome count, reaching a mean of 78.8 GB and 709.1 MB, respectively, for the largest datasets (10 000 genomes). Similarly, for both *Goalign* and *TrimAl*, generating a 95% core threshold alignment resulted in increased RAM usage proportional to genome count, reaching a mean of 4.2 GB and 2.3 GB, respectively, for the largest datasets. *Goalign* loads the whole alignment into memory, which allows it to be used in a Unix pipe (accept input via stdin) but increases RAM usage. The other tools cannot operate in a pipe as they require multiple passes over the file.

## DISCUSSION

This study highlights the importance of considering soft-core strategies as a best practice for phylogenetic analyses of bacterial datasets. Our findings reveal the limitations of using a strict- (100%) core threshold, particularly for large and diverse datasets, where even a slight relaxation from a 100% core to 99% notably increases the number of output sites. A 95% core emerges as a practical choice for many scenarios, striking a balance between retaining informative phylogenetic signals and excluding

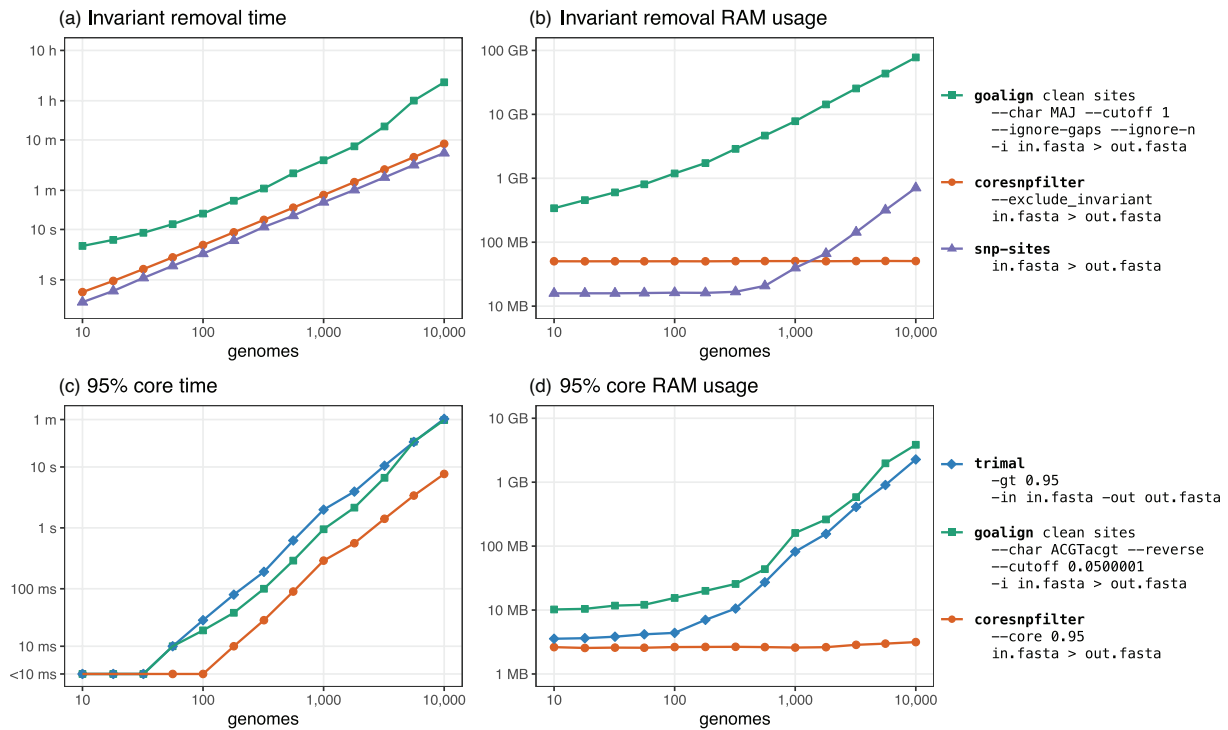


**Fig. 4.** Benchmarking of *Core-SNP-filter* against other tools with similar functionality. The time taken (a) and RAM usage (b) to remove invariant sites from alignments with varying numbers of genomes using three different tools (*Goalign*, *Core-SNP-filter* and *SNP-sites*). The time taken (c) and RAM usage (d) to generate a 95% core alignment across alignments with varying numbers of genomes using three different tools (*TrimAl*, *Goalign* and *Core-SNP-filter*). All axes are transformed with a log scale.

data inconsistent with the clonal frame of evolution or influenced by recombination. We also benchmarked the computational performance of our tool, *Core-SNP-filter*, against available tools that perform part, or all, of the required processing, demonstrating its efficiency in handling large datasets.

Traditional methods often rely on generating strict alignments from all genomes in a dataset as the basis for phylogenetic inferences and genomics evolutionary studies. However, as we demonstrate, this approach becomes increasingly impractical and ineffective as datasets grow. The strict-core method, which requires the alignment of SNPs present in all genomes, often results in significant data loss, reducing the resolution and accuracy of phylogenetic analyses. Recent studies have explored alternative methods for generating phylogenies from large bacterial datasets, including concatenated core genome multilocus sequence typing alignments and neighbour-joining trees based on pairwise core-SNP distances [19, 80, 81]. While these methods address some challenges, our study presents a simple tool striking a balance between traditional strict-core approaches and addressing present limitations. These soft-core approaches are being implemented in a number of large-scale phylogenetic studies [6, 26, 27].

In public health and hospital outbreak settings, phylogenetic analysis is crucial for inferring transmission dynamics. Typically, SNP distances calculated from strict-core alignments are used to determine transmission clusters. However, this method can be problematic due to its sensitivity to reference genome selection, masking of recombinogenic or prophage regions, and the approach taken [23]. These issues are exacerbated in large datasets, where a static SNP-distance threshold for transmission clustering may be inappropriate. Such thresholds, while standard in many transmission studies and accredited pipelines, fail to account for dynamic core sizes that result from strict-core approaches, particularly in epidemiological studies involving expanding datasets [82–84]. Our findings indicate that as datasets expand, the alignment size diminishes under a strict-core threshold, potentially leading to over-supported transmission networks and misleading clinical or public health conclusions. Moreover, the use of a strict-core approach resulted in a higher proportion of identical genome pairs across multiple studies, suggesting a loss of resolution that could obscure important genetic distinctions. This reduced resolution may impact decisions in outbreak response, where the ability to detect subtle genetic differences is essential for accurate transmission inference. By relaxing the core threshold, stable alignment sizes can be maintained up to and likely beyond 10 000 genomes, improving phylogenetic accuracy without compromising data integrity.

Furthermore, the strict-core approach poses challenges when generating whole-genome alignments from enrichment or capture-based methods, which are valuable for sequencing unculturable pathogens but often result in higher rates of missing data.

These enrichment and capture-based methods are relatively new and are being used more frequently for bacteria, necessitating the establishment of best-practice data analysis techniques [6, 11, 85, 86]. Similarly, missing data may arise when sequencing viral genomes, especially when genomes are sequenced directly from clinical samples. The inherent diversity of viruses and the often degraded nature of clinical samples exacerbate the problem, making it more challenging to achieve complete sequencing coverage [87]. As a result, adjustments to account for missing data have become more prevalent in viral and enrichment WGS data, driving the adoption of more adaptable analytical methods. For these datasets, a soft-core approach conserves data that are part of the clonal frame of evolution but sometimes fail to sequence [88]. To address this issue, enrichment and viral studies have started to adopt soft-core methods using alternative tools, highlighting the need for more flexible approaches to preserve critical genomic information [6, 11].

For datasets with a strong temporal signal and limited geographic diversity, discarding SNP positions using a strict-core threshold can remove information used by phylodynamic analyses. A soft-core approach can be valuable here and complement other tools such as *Gubbins* for recombination filtering. Our analysis showed that for recombination-unfiltered alignments, a 95% core threshold generally performs better (e.g. *Streptococcus pneumoniae* and *N. gonorrhoeae*) or similarly (e.g. *Staphylococcus aureus* and *Salmonella* Kentucky) to a 100% core threshold, making 95% the preferred threshold. Lower thresholds sometimes performed worse on unfiltered alignments due to recombinant regions. In our *Staphylococcus aureus* dataset, for instance, one isolate (SAMEA3212906) appeared as an outlier on a long branch in the root-to-tip regression at lower thresholds (<92%), whereas higher thresholds (>92%) helped to isolate the phylogenetic signal. For recombination-filtered alignments, the core threshold showed little impact on temporal signal values, except for sometimes causing a clear decline near 100%. Thresholds ranging from 50 to 95% performed similarly, suggesting that overly strict cores discard valuable data. For example, our recombination-filtered *N. gonorrhoeae* dataset lost over 90% of SNPs at a 100% core threshold. Overall, a 95% core threshold generally outperforms a 100% threshold.

The impact of missing data on phylogenetic inference has been a topic of significant ongoing debate, with studies showing contrasting views [24, 25, 89, 90]. Several studies find that minimal missing data does not substantially affect phylogenetic outcomes, especially in large datasets where missing data is proportionally low [25, 89]. However, other studies indicate that higher levels of missing data, such as >50% of sites, can introduce uncertainty in inferred topologies and result in misleading branch lengths [24, 90]. A further consideration is the datasets used to explore this question, which range from short alignments of 18S and 28S rRNA from tapeworms to long alignments in the thousands for brush-tongued parrots [24, 25]. Overall, these studies debate the utility of including some missing data in datasets of differing scale and origin. Here, we instead focus on the fundamental point that including sites with some gaps provides additional phylogenetic information for those samples where the site is known. We show that phylogenetic trees constructed from a 95% core threshold alignment can result in better-resolved topologies than those from 100% core threshold alignments. In the context of Felsenstein's pruning algorithm, which underpins likelihood-based phylogenetics, sites with some gaps carry information to resolve relationships between samples for which a base is present that would otherwise be discarded under a 100% core threshold, while gaps do not reduce the information offered by these terms [91]. Depending on the data at hand, additional sites with some gaps may serve to make estimated branch lengths and topology more or less certain, depending on the likelihoods of a branch length or a given topology at sites including gaps. Thus, our approach of using a 95% core threshold can result in better-resolved topologies, particularly in large-scale bacterial datasets.

When comparing *Core-SNP-filter* to other tools with similar capabilities, the choice of tool has minimal impact on small datasets (e.g. <100 samples), as all tested tools are sufficiently fast and efficient. However, for large datasets (e.g. >1000 samples), especially those containing invariant sites, both time and RAM become critical factors, and *Core-SNP-filter* has the potential to scale to very large datasets (e.g. >100 000 samples). *Goalign* presents challenges due to its non-intuitive commands for excluding invariant sites and producing soft-core alignments, though it has functionality for processing alignments in ways that *Core-SNP-filter* cannot.

Our study underscores the advantages of using soft-core thresholds, particularly the 95% threshold, over 100% strict-core thresholds for bacterial genome datasets. The soft-core approach, achieved with *Core-SNP-filter*, preserves more informative sites, enhancing phylogenetic resolution and temporal signals, while being computationally efficient. Researchers and public health professionals should consider using a soft core in their analyses to retain available evolutionary signals and accurately interpret phylogenetic relationships and transmission patterns.

---

#### Funding information

MLT is supported by an Australian Government Research Training Program Scholarship. DJI is supported by an National Health and Medical Research Council of Australia (NHMRC) Investigator Grant (GNT1195210). TPS is supported by an NHMRC Investigator Grant (GNT1194325).

#### Author contributions

M.L.T., R.R.W., G.T. and L.A.F. designed the study. M.L.T. and R.R.W. performed all analyses. M.L.T., R.R.W., T.S., G.T. and L.A.F. prepared the figures. G.T., D.J.I., T.S. and T.P.S. provided supervision and support. The first draft of the manuscript was written by M.L.T., being revised by all authors. All authors had full access to all study data. The corresponding authors had final responsibility for the decision to submit for publication.

**Conflicts of interest**

The authors declare that there are no conflicts of interest.

**Ethical statement**

No ethics approval was required for this study.

**References**

- Wooding S. Inferring phylogenies. *Am J Hum Genet* 2004;74:1074.
- Attwood SW, Hill SC, Aanensen DM, Connor TR, Pybus OG. Phylogenetic and phylodynamic approaches to understanding and combating the early SARS-CoV-2 pandemic. *Nat Rev Genet* 2022;23:547–562.
- Colijn C, Gardy J. Phylogenetic tree shapes resolve disease transmission patterns. *Evol Med Public Health* 2014;2014:96–108.
- Lane CR, Sherry NL, Porter AF, Duchene S, Horan K, et al. Genomics-informed responses in the elimination of COVID-19 in Victoria, Australia: an observational, genomic epidemiological study. *Lancet Public Health* 2021;6:e547–e556.
- Seemann T, Lane CR, Sherry NL, Duchene S, Gonçalves da Silva A, et al. Tracking the COVID-19 pandemic in Australia using genomics. *Nat Commun* 2020;11:4376.
- Taouk ML, Taiaroa G, Pasricha S, Herman S, Chow EPF, et al. Characterisation of *Treponema pallidum* lineages within the contemporary syphilis outbreak in Australia: a genomic epidemiological analysis. *Lancet Microbe* 2022;3:e417–e426.
- Williamson DA, Chow EPF, Gorrie CL, Seemann T, Ingle DJ, et al. Bridging of *Neisseria gonorrhoeae* lineages across sexual networks in the HIV pre-exposure prophylaxis era. *Nat Commun* 2019;10:3988.
- Croucher NJ, Page AJ, Connor TR, Delaney AJ, Keane JA, et al. Rapid phylogenetic analysis of large samples of recombinant bacterial whole genome sequences using Gubbins. *Nucleic Acids Res* 2015;43:e15–e.
- Didelot X, Wilson DJ. ClonalFrameML: efficient inference of recombination in whole bacterial genomes. *PLoS Comput Biol* 2015;11:e1004041.
- Baines SL, Holt KE, Schultz MB, Seemann T, Howden BO, et al. Convergent adaptation in the dominant global hospital clone ST239 of methicillin-resistant *Staphylococcus aureus*. *mBio* 2015;6:e00080.
- Beale MA, Marks M, Cole MJ, Lee M-K, Pitt R, et al. Global phylogeny of *Treponema pallidum* lineages reveals recent expansion and spread of contemporary syphilis. *Nat Microbiol* 2021;6:1549–1560.
- Gorrie CL, Mirčeta M, Wick RR, Judd LM, Lam MMC, et al. Genomic dissection of *Klebsiella pneumoniae* infections in hospital patients reveals insights into an opportunistic pathogen. *Nat Commun* 2022;13:3017.
- Hawkey J, Le Hello S, Doublet B, Granier SA, Hendriksen RS, et al. Global phylogenomics of multidrug-resistant *Salmonella enterica* serotype Kentucky ST198. *Microb Genom* 2019;5:e000269.
- Ingle DJ, Ambrose RL, Baines SL, Duchene S, Gonçalves da Silva A, et al. Evolutionary dynamics of multidrug resistant *Salmonella enterica* serovar 4,[5],12:i:- in Australia. *Nat Commun* 2021;12:4786.
- Ingle DJ, Andersson P, Valcanis M, Barnden J, Agd S, et al. Prolonged outbreak of multidrug-resistant *Shigella sonnei* harboring bla sub CTX-M-27 in Victoria, Australia. *Antimicrob Agents Chemother* 2020;64:01518–01520.
- Thomas JC, Seby S, Abrams AJ, Cartee J, Lucking S, et al. Evidence of recent genomic evolution in Gonococcal strains with decreased susceptibility to cephalosporins or azithromycin in the United States, 2014–2016. *J Infect Dis* 2019;220:294–305.
- Golparian D, Harris SR, Sánchez-Busó L, Hoffmann S, Shafer WM, et al. Genomic evolution of *Neisseria gonorrhoeae* since the preantibiotic era (1928–2013): antimicrobial use/misuse selects for resistance and drives evolution. *BMC Genom* 2020;21:116.
- Satam H, Joshi K, Mangrolia U, Waghoo S, Zaidi G, et al. Next-generation sequencing technology: current trends and advancements. *Biology* 2023;12:997.
- Carey ME, Dyson ZA, Ingle DJ, Amir A, Aworh MK, et al. Global diversity and antimicrobial resistance of typhoid fever pathogens: insights from a meta-analysis of 13,000 *Salmonella* Typhi genomes. *eLife* 2023;12:e85867.
- Harrison OB, Cehovin A, Skett J, Jolley KA, Massari P, et al. *Neisseria gonorrhoeae* population genomics: use of the gonococcal core genome to improve surveillance of antimicrobial resistance. *J Infect Dis* 2020;222:1816–1825.
- Higgs C, Sherry NL, Seemann T, Horan K, Walpola H, et al. Optimising genomic approaches for identifying vancomycin-resistant *Enterococcus faecium* transmission in healthcare settings. *Nat Commun* 2022;13:509.
- Mason LCE, Greig DR, Cowley LA, Partridge SR, Martinez E, et al. The evolution and international spread of extensively drug resistant *Shigella sonnei*. *Nat Commun* 2023;14:1983.
- Gorrie CL, Da Silva AG, Ingle DJ, Higgs C, Seemann T, et al. Key parameters for genomics-based real-time detection and tracking of multidrug-resistant bacteria: a systematic analysis. *Lancet Microbe* 2021;2:e575–e583.
- Smith BT, Mauck WM III, Benz BW, Andersen MJ. Uneven missing data skew phylogenomic relationships within the Lories and Lorikeets. *Genome Biol Evol* 2020;12:1131–1147.
- Jacob Machado D, Castroviejo-Fisher S, Grant T. Evidence of absence treated as absence of evidence: the effects of variation in the number and distribution of gaps treated as missing data on the results of standard maximum likelihood analysis. *Mol Phylogenet Evol* 2021;154:106966.
- Fitzpatrick MA, Ozer EA, Hauser AR. Utility of whole-genome sequencing in characterizing acinetobacter epidemiology and analyzing hospital outbreaks. *J Clin Microbiol* 2016;54:593–612.
- Giulieri SG, Guérrillot R, Holmes NE, Baines SL, Hachani A, et al. A statistical genomics framework to trace bacterial genomic predictors of clinical outcomes in *Staphylococcus aureus* bacteremia. *Cell Rep* 2023;42:113069.
- Argimón S, David S, Underwood A, Abrudan M, Wheeler NE, et al. Rapid genomic characterization and global surveillance of *Klebsiella* using pathogenwatch. *Clin Infect Dis* 2021;73:S325–S335.
- Hamilton HL, Dillard JP. Natural transformation of *Neisseria gonorrhoeae*: from DNA donation to homologous recombination. *Mol Microbiol* 2006;59:376–385.
- Kothapalli S, Nair S, Alokam S, Pang T, Khakhria R, et al. Diversity of genome structure in *Salmonella enterica* serovar Typhi populations. *J Bacteriol* 2005;187:2638–2650.
- Chung GT, Yoo JS, Oh HB, Lee YS, Cha SH, et al. Complete genome sequence of *Neisseria gonorrhoeae* NCCP11945. *J Bacteriol* 2008;190:6035–6036.
- Parkhill J, Dougan G, James KD, Thomson NR, Pickard D, et al. Complete genome sequence of a multiple drug resistant *Salmonella enterica* serovar Typhi CT18. *Nature* 2001;413:848–852.
- Alfsnes K, Eldholm V, Olsen AO, Brynildsrud OB, Bohlin J, et al. Genomic epidemiology and population structure of *Neisseria gonorrhoeae* in Norway, 2016–2017. *Microb Genom* 2020;6:e000359.
- Buckley C, Forde BM, Trembizki E, Lahra MM, Beatson SA, et al. Use of whole genome sequencing to investigate an increase in *Neisseria gonorrhoeae* infection among women in urban areas of Australia. *Sci Rep* 2018;8:1503.

35. Cehovin A, Harrison OB, Lewis SB, Ward PN, Ngetsa C, et al. Identification of novel *Neisseria gonorrhoeae* lineages harboring resistance plasmids in Coastal Kenya. *J Infect Dis* 2018;218:801–808.
36. DeSilva D, Peters J, Cole K, Cole MJ, Cresswell F, et al. Whole-genome sequencing to determine transmission of *Neisseria gonorrhoeae*: an observational study. *Lancet Infect Dis* 2016;16:1295–1303.
37. Demczuk W, Lynch T, Martini, VanDomselaar G, Graham M, et al. Whole-genome phylogenomic heterogeneity of *Neisseria gonorrhoeae* isolates with decreased cephalosporin susceptibility collected in Canada between 1989 and 2013. *J Clin Microbiol* 2015;53:191–200.
38. Didelot X, Dordel J, Whittles LK, Collins C, Bilek N, et al. Genomic analysis and comparison of two gonorrhoea outbreaks. *mBio* 2016;7:e00525-16.
39. Ezewudo MN, Joseph SJ, Castillo-Ramirez S, Dean D, Del Rio C, et al. Population structure of *Neisseria gonorrhoeae* based on whole genome data and its relationship with antibiotic resistance. *PeerJ* 2015;3:e806.
40. Fifer H, Saunders J, Soni S, Sadiq ST, FitzGerald M. 2018 UK national guideline for the management of infection with *Neisseria gonorrhoeae*. *Int J STD AIDS* 2020;31:4–15.
41. Grad YH, Harris SR, Kirkcaldy RD, Green AG, Marks DS, et al. Genomic Epidemiology of gonococcal resistance to extended-spectrum cephalosporins, macrolides, and fluoroquinolones in the United States, 2000–2013. *J Infect Dis* 2016;214:1579–1587.
42. Kwong JC, Chow EPF, Stevens K, Stinear TP, Seemann T, et al. Whole-genome sequencing reveals transmission of gonococcal antibiotic resistance among men who have sex with men: an observational study. *Sex Transm Infect* 2018;94:151–157.
43. Kwong JC, Gonçalves da Silva A, Dyet K, Williamson DA, Stinear TP, et al. NGMASTER: in silico multi-antigen sequence typing for *Neisseria gonorrhoeae*. *Microb Genom* 2016;2:e000076.
44. Lan PT, Golparian D, Ringlander J, Van Hung L, Van Thuong N, et al. Genomic analysis and antimicrobial resistance of *Neisseria gonorrhoeae* isolates from Vietnam in 2011 and 2015–16. *J Antimicrob Chemother* 2020;75:1432–1438.
45. Lee RS, Seemann T, Heffernan H, Kwong JC, Gonçalves da Silva A, et al. Genomic epidemiology and antimicrobial resistance of *Neisseria gonorrhoeae* in New Zealand. *J Antimicrob Chemother* 2018;73:353–364.
46. Mortimer TD, Pathela P, Crawley A, Rakeman JL, Lin Y, et al. The distribution and spread of susceptible and resistant *Neisseria gonorrhoeae* across demographic groups in a major metropolitan center. *Clin Infect Dis* 2021;73:e3146–e3155.
47. Ryan L, Golparian D, Fennelly N, Rose L, Walsh P, et al. Antimicrobial resistance and molecular epidemiology using whole-genome sequencing of *Neisseria gonorrhoeae* in Ireland, 2014–2016: focus on extended-spectrum cephalosporins and azithromycin. *Eur J Clin Microbiol Infect Dis* 2018;37:1661–1672.
48. Sánchez-Busó L, Golparian D, Corander J, Grad YH, Ohnishi M, et al. The impact of antimicrobials on gonococcal evolution. *Nat Microbiol* 2019;4:1941–1950.
49. Town K, Field N, Harris SR, Sánchez-Busó L, Cole MJ, et al. Phylogenomic analysis of *Neisseria gonorrhoeae* transmission to assess sexual mixing and HIV transmission risk in England: a cross-sectional, observational, whole-genome sequencing study. *Lancet Infect Dis* 2020;20:478–486.
50. Wind CM, de Vries E, Schim van der Loeff MF, van Rooijen MS, van Dam AP, et al. Decreased azithromycin susceptibility of *Neisseria gonorrhoeae* isolates in patients recently treated with azithromycin. *Clin Infect Dis* 2017;65:37–45.
51. Yahara K, Nakayama S-I, Shimuta K, Lee K-I, Morita M, et al. Genomic surveillance of *Neisseria gonorrhoeae* to investigate the distribution and evolution of antimicrobial-resistance determinants and lineages. *Microb Genom* 2018;4:e000205.
52. Argimón S, Nagaraj G, Shamanna V, Sravani D, Vasanth AK, et al. Circulation of third-generation cephalosporin resistant *Salmonella* Typhi in Mumbai, India. *Clin Infect Dis* 2022;74:2234–2237.
53. Ashton PM, Nair S, Peters TM, Bale JA, Powell DG, et al. Identification of *Salmonella* for public health surveillance using whole genome sequencing. *PeerJ* 2016;4:e1752.
54. Carey ME, Thi Nguyen TN, Tran DHN, Dyson ZA, Keane JA, et al. The origins of haplotype 58 (H58) *Salmonella enterica* serovar Typhi. *Commun Biol* 2024;7:775.
55. Chattaway MA, Gentle A, Nair S, Tingley L, Day M, et al. Phylogenomics and antimicrobial resistance of *Salmonella* Typhi and Paratyphi A, B and C in England, 2016–2019. *Microb Genom* 2021;7:000633.
56. da Silva KE, Tanmoy AM, Pragasam AK, Iqbal J, Sajib MSI, et al. The international and intercontinental spread and expansion of antimicrobial-resistant *Salmonella* Typhi a genomic epidemiology study. *Lancet Microbe* 2022;3:e567–e577.
57. Gauld JS, Olgemoeller F, Heinz E, Nkhata R, Bilima S, et al. Spatial and genomic data to characterize endemic typhoid transmission. *Clin Infect Dis* 2022;74:1993–2000.
58. Guevara PD, Maes M, Thanh DP, Duarte C, Rodriguez EC, et al. A genomic snapshot of *Salmonella enterica* serovar Typhi in Colombia. *PLoS Negl Trop Dis* 2021;15:e0009755.
59. Ingle DJ, Nair S, Hartman H, Ashton PM, Dyson ZA, et al. Informal genomic surveillance of regional distribution of *Salmonella* Typhi genotypes and antimicrobial resistance via returning travellers. *PLoS Negl Trop Dis* 2019;13:e0007620.
60. Kariuki S, Dyson ZA, Mbae C, Ngetich R, Kavai SM, et al. Multiple introductions of multidrug-resistant typhoid associated with acute infection and asymptomatic carriage, Kenya. *eLife* 2021;10:e67852.
61. Klemm EJ, Shakoor S, Page AJ, Qamar FN, Judge K, et al. Emergence of an extensively drug-resistant *Salmonella enterica* Serovar Typhi clone harboring a promiscuous plasmid encoding resistance to fluoroquinolones and third-generation cephalosporins. *mBio* 2018;9:e00105-18.
62. Maes M, Sikorski MJ, Carey ME, Higginson EE, Dyson ZA, et al. Whole genome sequence analysis of *Salmonella* Typhi provides evidence of phylogenetic linkage between cases of typhoid fever in Santiago, Chile in the 1980s and 2010–2016. *PLoS Negl Trop Dis* 2022;16:e0010178.
63. Park SE, Pham DT, Boinett C, Wong VK, Pak GD, et al. The phylogeography and incidence of multi-drug resistant typhoid fever in sub-Saharan Africa. *Nat Commun* 2018;9:5094.
64. Pragasam AK, Pickard D, Wong V, Dougan G, Kang G, et al. Phylogenetic analysis indicates a longer term presence of the globally distributed H58 haplotype of *Salmonella* Typhi in southern India. *Clin Infect Dis* 2020;71:1856–1863.
65. Rahman SIA, Dyson ZA, Klemm EJ, Khanam F, Holt KE, et al. Population structure and antimicrobial resistance patterns of *Salmonella* Typhi isolates in urban Dhaka, Bangladesh from 2004 to 2016. *PLoS Negl Trop Dis* 2020;14:e0008036.
66. Rasheed F, Saeed M, Alikhan N-F, Baker D, Khurshid M, et al. Emergence of resistance to fluoroquinolones and third-generation cephalosporins in *Salmonella* Typhi in Lahore, Pakistan. *Microorganisms* 2020;8:1336.
67. Tanmoy AM, Westeel E, De Bruyne K, Goris J, Rajoharison A, et al. *Salmonella enterica* Serovar Typhi in Bangladesh: exploration of genomic diversity and antimicrobial resistance. *mBio* 2018;9:e02112-18.
68. Thilliez G, Mashe T, Chaibva BV, Robertson V, Bawn M, et al. Population structure and evolution of *Salmonella enterica* serotype Typhi in Zimbabwe before a typhoid conjugate vaccine immunization campaign. *bioRxiv*; 2022;2022.
69. Wong VK, Baker S, Pickard DJ, Parkhill J, Page AJ, et al. Phylogeographical analysis of the dominant multidrug-resistant H58 clade of *Salmonella* Typhi identifies inter- and intracontinental transmission events. *Nat Genet* 2015;47:632–639.
70. Croucher NJ, Harris SR, Fraser C, Quail MA, Burton J, et al. Rapid pneumococcal evolution in response to clinical interventions. *Science* 2011;331:430–434.

71. Nguyen L-T, Schmidt HA, von Haeseler A, Minh BQ. IQ-TREE: a fast and effective stochastic algorithm for estimating maximum-likelihood phylogenies. *Mol Biol Evol* 2015;32:268–274.
72. Paradis E, Schliep K. ape 5.0: an environment for modern phylogenetics and evolutionary analyses in R. *Bioinformatics* 2019;35:526–528.
73. Robinson DF, Foulds LR (eds). *Comparison of Weighted Labelled Trees*. 1979.
74. Schliep KP. phangorn: phylogenetic analysis in R. *Bioinformatics* 2011;27:592–593.
75. Capella-Gutiérrez S, Silla-Martínez JM, Gabaldón T. trimAl: a tool for automated alignment trimming in large-scale phylogenetic analyses. *Bioinformatics* 2009;25:1972–1973.
76. Lemoine F, Gascuel O. Gtree/Goalign: toolkit and Go API to facilitate the development of phylogenetic workflows. *NAR Genom Bioinform* 2021;3:lqab075.
77. Page AJ, Taylor B, Delaney AJ, Soares J, Seemann T, et al. *SNP-sites*: rapid efficient extraction of SNPs from multi-FASTA alignments. *Microb Genom* 2016;2:e000056.
78. Biek R, Pybus OG, Lloyd-Smith JO, Didelot X. Measurably evolving pathogens in the genomic era. *Trends Ecol Evol* 2015;30:306–313.
79. Featherstone LA, Zhang JM, Vaughan TG, Duchene S. Epidemiological inference from pathogen genomes: a review of phylodynamic models and applications. *Virus Evol* 2022;8:veac045.
80. Hennart M, Guglielmini J, Bridel S, Maiden MCJ, Jolley KA, et al. A dual barcoding approach to bacterial strain nomenclature: genomic taxonomy of *Klebsiella pneumoniae* strains. *Mol Biol Evol* 2022;39:msac135.
81. Taouk ML, Tairaoa G, Duchene S, Low SJ, Higgs CK, et al. Longitudinal genomic analysis of *Neisseria gonorrhoeae* transmission dynamics in Australia. *Nat Commun* 2024;15:8076.
82. Jajou R, Kohl TA, Walker T, Norman A, Cirillo DM, et al. Towards standardisation: comparison of five whole genome sequencing (WGS) analysis pipelines for detection of epidemiologically linked tuberculosis cases. *Euro Surveill* 2019;24:1900130.
83. Mixão V, Pinto M, Sobral D, Di Pasquale A, Gomes JP, et al. ReporTree: a surveillance-oriented tool to strengthen the linkage between pathogen genetic clusters and epidemiological data. *Genome Med* 2023;15:43.
84. Stimson J, Gardy J, Mathema B, Crudu V, Cohen T, et al. Beyond the SNP threshold: identifying outbreak clusters using inferred transmissions. *Mol Biol Evol* 2019;36:587–603.
85. Depledge DP, Palser AL, Watson SJ, Lai IY-C, Gray ER, et al. Specific capture and whole-genome sequencing of viruses from clinical samples. *PLoS One* 2011;6:e27805.
86. Mee PT, Buultjens AH, Oliver J, Brown K, Crowder JC, et al. Mosquitoes provide a transmission route between possums and humans for Buruli ulcer in southeastern Australia. *Nat Microbiol* 2024;9:377–389.
87. Martin GE, Tairaoa G, Taouk ML, Savic I, O'Keefe J, et al. Maintaining genomic surveillance using whole-genome sequencing of SARS-CoV-2 from rapid antigen test devices. *Lancet Infect Dis* 2022;22:1417–1418.
88. Taouk ML, Steinig E, Tairaoa G, Savic I, Tran T, et al. Intra- and interhost genomic diversity of monkeypox virus. *J Med Virol* 2023;95:e29029.
89. Dessimoz C, Gil M. Phylogenetic assessment of alignments reveals neglected tree signal in gaps. *Genome Biol* 2010;11:R37.
90. Lemmon AR, Brown JM, Stanger-Hall K, Lemmon EM. The effect of ambiguous data on phylogenetic estimates obtained by maximum likelihood and Bayesian inference. *Syst Biol* 2009;58:130–145.
91. Felsenstein J. Evolutionary trees from DNA sequences: a maximum likelihood approach. *J Mol Evol* 1981;17:368–376.

**The Microbiology Society is a membership charity and not-for-profit publisher.**

**Your submissions to our titles support the community – ensuring that we continue to provide events, grants and professional development for microbiologists at all career stages.**

**Find out more and submit your article at [microbiologyresearch.org](https://microbiologyresearch.org)**